Distributed Detection of Optical Radiation using Chirped-Pulse Phase-Sensitive Optical Time Domain Reflectometry

Regina Magalhães[1*], Andres Garcia-Ruiz[1], Hugo F. Martins[1], João Pereira[2], Walter Margulis[2], Sonia Martin-Lopez[1], and Miguel González-Herráez[1]

[1]*Dpto. de Electrónica, University of Alcalá, 28805, Alcalá de Henares (Madrid), Spain*

[2]*Acreo, Electrum 236, 16440, Stockholm, Sweden*

**regina.magalhaes@uah.es*

Abstract: A distributed bolometer operating over transparent-coated and carbon-coated optical fibers is proposed. The detection of light with irradiance sensitivities of in the order of 1% of the reference solar irradiance is readily demonstrated.

OCIS codes: (280.4788) Optical sensing and sensors; (290.5870) Scattering, Rayleigh; (190.4870) Photothermal effects

1. Introduction

Distributed Fiber Optic Sensors (DFOS) are capable of performing position-resolved measurements of physical variables (such as temperature, strain, pressure, etc) along a continuous optical fiber cable laid along a monitored element. These sensors conveniently replace thousands of independent detectors (discretely disposed along the structure to be monitored) with a single optical fiber cable and a single interrogation unit. In these cases, DFOS allow to reduce the overall energy consumption, the complexity, and also the cost of the monitoring system, especially when a very large number of detecting points is intended. In many applications, DFOS have not only proved to be a cost-effective solution, but also a very reliable monitoring tool (e.g. in pipeline monitoring) [1], particularly for the monitoring over very long distances (tens of kilometers). The interrogation schemes in these sensors rely on time or frequency-domain measurements of backscattering processes in the optical fiber, which can be originated by Rayleigh, Brillouin or Raman scattering. Since these processes only depend on temperature and/or strain, DFOS are particularly well suited for the distributed measurement of solely these two physical quantities. Thus, distributed measurement of other quantities becomes challenging as it typically requires some kind of transducing layer, to convert the targeted quantity into a temperature or strain change in the fiber core.

DFOS sensors have been extensively applied in monitoring power lines [2]. Typically, the main interest is the monitoring of hot spots in the power line, to prevent failures related to high-temperature degradation in the conductors. In applications like Dynamic Line Ratings (DLR) forecasting, it was reported that solar radiation can considerably increase the temperature of the conductor in low wind speed conditions, becoming a significant limiting factor [3]. In this scenario it was also reported that the solar radiation should be dynamically and continuously monitored along the conductor, since a single-point measurement of effective incident radiation would not be sufficient to compute the global combined effect of solar irradiance along the whole span. Surpassing the lack of available distributed radiation sensing technologies in DLR forecasting would therefore allow to overcome important limitations in this field.

Photothermal radiation measurements are a potential route to overcome this lack. Single-point fiber-tip photothermal sensors have been developed to measure optical radiation [4]. However, the extension of these concepts to distributed sensing is challenging. One could think on a high emissivity coating of a conventional fiber-optic cable. However, temperature resolutions of conventional Brillouin-based DFOS are typically around 1 K [1]. Considering the expectable temperature increase in the fiber due to the absorbed radiation in the earth surface, this would yield an approach with very poor sensitivity and little practicality. Recently, the use of phase-sensitive optical time domain reflectometry with linearly chirped pulses (CP-ΦOTDR) has been demonstrated to achieve robust, fast (kHz) and high sensitivity (mK) distributed fiber temperature measurements over distances of up to 70 km [5,6]. This is the starting point of our work. Here, we make the proof-of-concept of a distributed visible radiation sensor, operating as a distributed bolometer interrogated by a CP-ΦOTDR. The proposed method readily achieves a resolution compatible with solar radiation detection (≈1% of the reference solar spectral irradiance on earth), thus opening the door for important applications in industries related to solar radiation.

2. Bolometers and the proposed operation

2.1. Bolometer Principle of operation

A bolometer consists of an absorptive element weakly connected to a heat sink. The heat sink has a temperature T_0, assumed constant, while the absorber has a temperature $T(\geq T_0)$, which will depend on the incident irradiance, E_{inc}. If $E_{inc}=0$ (without incident irradiance), then $T=T_0$. However, when $E_{inc}>0$, the

absorber will absorb an optical power $P_{abs} = E_{inc} \cdot A_{inc} \cdot \alpha$, which depends on the absorber area of radiation incidence, A_{inc}, and an absorption coefficient of the absorber, α. Consequently, T will increase to $T > T_0$. In these conditions, the absorber will dissipate power to the heat sink, as described by Newton's law of cooling (assuming small temperature differences $T - T_0$) [7]:

$$P_{dissipated} = h \cdot A \cdot (T - T_0) \quad (1)$$

Where h is the heat transfer coefficient between the absorber and the heat sink and A is the heat transfer surface area. The system will then evolve to a thermal equilibrium state where $P_{abs} = P_{dissipated}$, over a transient time which will also depend on the absorber's heat capacity $C(T)$. For a given system, where all necessary constants are known, the incident radiation can then be calculated at the thermal equilibrium state using:

$$E_{inc} = (T - T_0) \cdot (h \cdot A)/(A_{inc} \cdot \alpha) = (T - T_0) / ¢ \quad (2)$$

Where ¢ is a constant which depends on the system parameters.

2.2. Proposed fiber based distributed Bolometer

In the system proposed in this work, an optical fiber is used as the absorbing element and the surrounding air as the heat sink. The temperature T of the optical fiber can be measured with millikelvin resolution using a CP-ΦOTDR, thus allowing for high sensitivities of the measurement of E_{inc}. However, the temperature of the surrounding air, T_0, is unknown. This problem is solved by using the difference between the temperature measurements of two optical fibers (assumed to be placed in the same environment and to receive the same irradiance), with different coatings, therefore presenting different optical absorption coefficients, α_1, α_2 (and/or different heat transfer coefficients h_1, h_2). In this case, the equilibrium state for fiber 1 and fiber 2 will be reached at different temperatures T_1, T_2:

$$E_{inc} = (T_1 - T_0) \cdot (h \cdot A)/(A_{inc} \cdot \alpha_1) = (T_1 - T_0) / ¢_1 \Leftrightarrow T_0 = T_1 - (E_{inc} \cdot ¢_1) \quad (3)$$

$$E_{inc} = (T_2 - T_0) \cdot (h \cdot A)/(A_{inc} \cdot \alpha_2) = (T_2 - T_0) / ¢_2 \Leftrightarrow T_0 = T_2 - (E_{inc} \cdot ¢_2) \quad (4)$$

By replacing $T_0 = T_1 - (E_{inc} \cdot ¢_1)$ in eq. 4, it is then derived that:

$$E_{inc} = (T_2 - T_1) / (¢_2 - ¢_1) \quad (5)$$

In other words, with the use of two fibers with different coating (and therefore different optical absorption coefficients), the measurement of an incident irradiance, E_{inc}, can be achieved simply by measuring the difference between the temperatures of the two fibers, for an arbitrary external temperature T_0. Note that the values of $¢_1$ and $¢_2$ are not really needed individually, but only the value of $(¢_2 - ¢_1)$, which can easily be calibrated by applying a known E_{inc} and measuring the resulting $(T_2 - T_1)$ in equilibrium.

3. Experimental Setup

The experimental setup used in this work for the proof-of-concept demonstration of a distributed bolometer is depicted in Figure 1. Two standard with different coatings (and, therefore, different absorption coefficients) are used as sensing elements. FUT1 was a transparent-coated fiber (lower absorption), while FUT2 was a carbon-painted fiber [8] (higher absorption). Both FUT had an outer diameter of 0.25 mm. Both FUTs had an overlapping section of ~10 m (the interrogator spatial resolution) which was wrapped in concentric circles with a radius of ~10 cm. This was made to ensure that both fibers would receive the same uniform irradiance, along at least the length of the interrogator spatial resolution. The two optical fibers are spliced together, as to achieve a single optical fiber to be monitored by the optical interrogator. The temperature of the two optical fibers was then measured in real-time by an optical distributed fiber temperature interrogator based on CP-ΦOTDR, as described below.

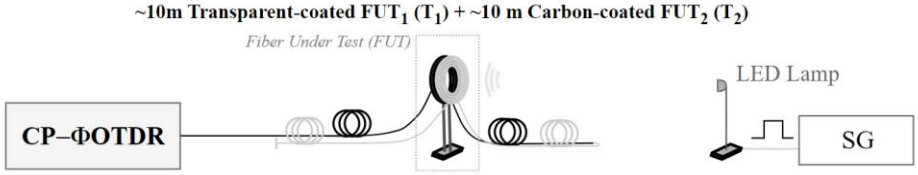

Fig. 1 - Experimental setup of the proposed fiber based distributed Bolometer.

Optical radiation was then applied to thes FUTs, using a visible LED lamp and an optical power output P_{LED} which could be varied by acting on the input voltage (up to 12 V) or the distance to the FUTs. The values of irradiance experienced by the FUTs were measured by a radiation pyrometer, with the detector placed at the position of the FUTs.

The interrogator used for the distributed temperature measurements was a CP-ΦOTDR, which allows for high sensitivity and fast distributed measurements of temperature. Detailed information on this measurement technique can be found in [5]. The CP-ΦOTDR measurement was performed using 100 ns pulses (corresponding to 10-meter spatial resolution), linearly chirped with ≈1 GHz of total pulse frequency content and a detection scheme enabling a temperature resolution of ≈2 mK, with a temperature sampling every 40 ms. Note that in this work a simple proof-of-concept demonstration of the distributed bolometer is intended. However, the experiment could be readily extended to the limits set by the temperature interrogation technique (CP-ΦOTDR): millikelvin resolutions over up to 70 km, with metric spatial resolution, capable of characterizing the temperature variations (the transient time between equilibrium stats) with sampling rates of kHz [6].

4. Visible Radiation Measurements

4.1. Demonstration of the principle of operation

To demonstrate the principle of visible radiation detection, the temperature of the two FUTs was monitored in the presence of different values of irradiance, (measured in real time by the radiation pyrometer). This was done by changing the distance of the LED to the FUTs, in five stages of 18 s each. The sequence of irradiance values was: (1) 0 W/m^2 (LED off), (2) 43.8 W/m^2, (3) 30.3 W/m^2, (4) 1.48 W/m^2, (5) 0 W/m^2 (LED off). Note that both FUT had a cross section area of ≈0.0025 m^2 over 10 m of fiber, i.e., the radiation power reaching the fibers varied between 0 mW up to 110 mW. The results obtained can be observed in Figure 2 for (a) the temperature shift of the FUTs (b) temperature difference between the FUTs.

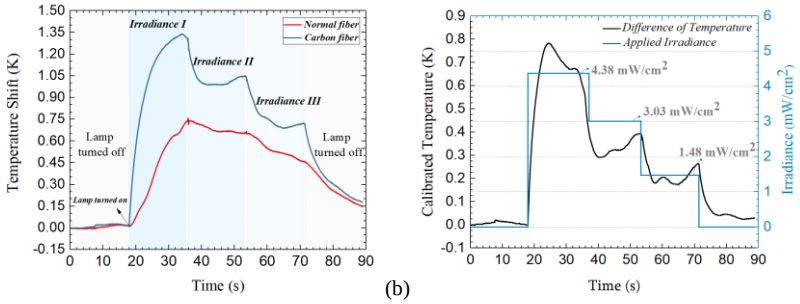

Fig. 2 – (a) Temperature shift experienced by the transparent-coated FUT (red line) and by the carbon-coated FUT (blue line), when submitted to irradiances of I ≈43.8 W/m^2 , II ≈30.3 W/m^2 and III ≈14.8 W/m^2 , at room temperature. **(b)** Correspondent temperature difference between the FUTs of figure (a), compared to the irradiance values applied.

The presented results in Figure 2 (b), clearly demonstrate the operation principle of the method, presenting a difference of temperature between FUT1 and FUT2, which varies for different applied irradiances, as expected from eq. 5. A value of $1/(¢_2\text{-}¢_1) \approx 66$ (Wm^{-2}K^{-1}) can be estimated from the results (see eq. 5). The error of the measurements presented in Fig. 2b (ratio between applied radiances and temperature shifts should be a constant) seems to be affected by the fact that the temperatures of the fibers do not reach a perfect equilibrium state in the 18 s between irradiance stages (chosen as to simulate field conditions). In any case, note that the step between the irradiances applied (≈15 W/m^2), corresponds to ≈1.5% of the reference solar spectral irradiance on earth at surface level ("Air Mass 1.5", defined as 1000 W/m by the "American Society for testing and materials" [9]).

4.2. System linearity for different applied irradiances and fiber absorption characterization

After demonstrating the principle of operation of the proposed distributed fiber bolometer, the system linearity was then characterized for varying irradiances applied to the fiber. This characterization was done in the transient regime (i.e., before the system reaches the thermal equilibrium). The driving motivation for the proposed method was that it additionally allows characterizing the absorption response of fibers individually (as described below). In order to characterize the system in the transient regime, the irradiance applied to the fiber was defined as a square wave (i.e., alternating "on" and "off" states), of a certain amplitude (i.e, the Irradiance amplitude on the "on" state). In this case, since thermal equilibrium is not reached, the fiber temperature will oscillate around a certain mean value. The amplitude of these temperature oscillations is expected to be linearly proportional to the applied irradiance amplitude, as this is proportional to the absorbed optical power ($P_{abs} = E_{inc} \cdot A_{inc} \cdot \alpha$, see introduction).

Note that the value of the amplitude of the temperature oscillations will depend on the period of the applied square function (since for longer periods, the fiber will be heated during longer times). Therefore, the "absolute" value of the temperature of the oscillations is not the important factor, but rather its variation when the

irradiance is varied, for a fixed period. For this reason, the amplitude of the temperature oscillations was normalized to 1 for an applied (square wave amplitude) irradiance of 10 W/m^2. The results are presented in Figure 3 and, as expected, the amplitude of the temperature oscillations were observed to have a linear dependence on the applied irradiance amplitudes, demonstrating the linearity of the technique.

An important application of this method is that it additionally allows to characterize the optical absorption coefficients (α in equation 2) of individual fibers separately. If the same irradiance amplitude is applied to different fibers (with a period of arbitrary value, as long as it is fixed and below the times at which the system reaches thermal equilibrium), then the amplitude of the fluctuations will provide a measurement proportional to the α of the fiber. Since the method proposed in 4.1 requires two fibers with different α, it is important to be able to characterize a set of N fibers individually (and rapidly), allowing for a choice of better sets of pairs of fibers to be used. Note that this measurement is inmune to drifts of the temperature of the surronding air, as the mean value of the temperature oscilations is not important, making this a robust procedure for fiber characterization to be used outside the laboratory.

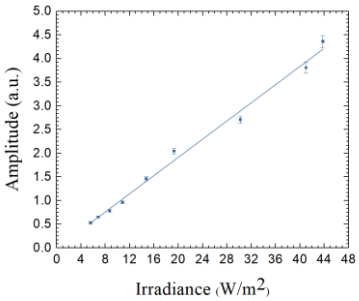

Fig. 3 – (a) Amplitude of the fiber temperature oscilations as a function of the applied Irradiance amplitude, for an applied irradiance defined as a square wave ("on", "off" state) with a period of 5s, applied to the carbon-coated fiber.

5. Conclusions

In this work, a proof-of-concept demonstration of the operation of a distributed bolometer operating over conventional optical fibers is presented, with promising results. It is based on measuring the temperature difference between two optical fibers with coatings of different optical absorption coefficients, without requiring knowledge of the surrounding temperature. A high sensitivity is achieved, taking advantage of the high temperature sensitivity (mK range) of the optical interrogator (CP-ΦOTDR). The sensor was readily demonstrated to be able to measure absolute values of irradiance with sensitivities of 10 W/m^2, equivalent to ≈1% of the reference solar spectral irradiance on earth at surface level, corresponding to temperature differences of ≈150 mK. The available sensitivities are compatible with the detection of solar radiation over tens of km with meter scale spatial resolutions. Thus, the proposed sensor has a high potential for integration in solar radiation-based applications, such as DLR forecasting, or photovoltaic industries. Further studies are also envisaged using different fiber coatings in order to achieve spectral discrimination (using coatings of different colors).

Acknowledgments

This work was supported by ITN-FINESSE, funded by the EU's Horizon 2020 research and innovation program under the Marie Sklodowska-Curie Action grant agreement n° 722509EU; the European Research Council through project U FINE (Grant307441); the European Commission through project MSCA-ITN-ETN-722509; the DOMINO Water JPI project, under the WaterWorks2014 cofounded call by EC Horizon 2020 and Spanish MINECO; the Spanish MINECO through project TEC2015-71127-C2-2-R and through a "Ramón y Cajal" contract.; and the regional program SINFOTON-CM: S2013/MIT-2790.

References

[1] X. Bao and L. Chen, "Recent progress in distributed fiber optic sensors," Sensors **12(7)**, 8601-8639 (2012).
[2] G. Yilmaz, S.E. Karlik, "A distributed optical fiber sensor for temperature detection in power cables," Sensor Actuat A-Phys **125**(2), 148-155, (2006)
[3] G.Y. Chen, X. Wu, X. Liu, D.G. Lancaster, T.M. Monro, H. Xu, "Photodetector based on Vernier-Enhanced Fabry-Perot Interferometers with a Photo-Thermal Coating," Scientific Reports, 7, art. no. 41895 (2017).
[4] A. Michiorri, H.M. Nguyen, S. Alessandrini, J.B. Bremnes, S. Dierer, E. Ferrero, B.E Nygaard, P. Pinson, N. Thomaidis and S. Uski, "Forecasting for dynamic line rating," Renewable and Sustainable Energy Reviews **52**, 1713-1730 (2015).
[5] J. Pastor-Graells, H.F. Martins, A. Garcia-Ruiz, S. Martin-Lopez and M. Gonzalez-Herraez, "Single-shot distributed temperature and strain tracking using direct detection phase-sensitive OTDR with chirped pulses," Opt. Express **24(12)**, 13121-13133 (2016).
[6] J. Pastor-Graells, J. Nuno, M.R. Fernandez-Ruiz, A. Garcia-Ruiz, H.F. Martins, S. Martin-Lopez, M. Gonzalez-Herraez, "Chirped-Pulse Phase-Sensitive Reflectometer Assisted by First-Order Raman Amplification," J. Lightwave Technol., 35 (21), 4677-4683 (2017).
[7] A. Garcia-Ruiz, J. Pastor-Graells, H.F. Martins, K.H. Tow, L. Thévenaz, S. Martin-Lopez and M. Gonzalez-Herraez, "Distributed photothermal spectroscopy in microstructured optical fibers: towards high-resolution mapping of gas presence over long distances," Opt. Express **25(3)**, 1789-805 (2017).
[8] A. Sudirman, L. Norin and W. Margulis, "Increased sensitivity in fiber-based spectroscopy using carbon-coated fiber," Opt. Express **20(27)**, 28049-55 (2012).
[9] ASTM, "Standard Tables for Reference Solar Spectral Irradiances: Direct Normal and Hemispherical on 37° Tilted Surface," E-892, Vol. 14.04., (2012).